



Characterization of the PON1 active site using modeling simulation, in relation to PON1 lactonase activity

Hagai Tavori^{a,b}, Soliman Khatib^a, Michael Aviram^b, Jacob Vaya^{a,*}

^aLaboratory of Natural Medicinal Compounds, MIGAL—Galilee Technology Center, PO Box 831, Kiryat Shmona 11016, and Tel Hai College, Israel

^bRappaport Family Institute for Research in the Medical Science, Rambam Medical Center, Haifa 31096, Israel

ARTICLE INFO

Article history:

Received 17 February 2008

Accepted 4 June 2008

Available online 12 June 2008

Keywords:

Docking

Lactones

Lactonization

Modeling

Paraoxonase1

ABSTRACT

Paraoxonase1 (PON1) is a HDL bound enzyme and many of the anti-atherogenic properties of HDL are attributed to PON1. The enzyme precise mechanism of protective action and its endogenous substrate remain elusive. PON1 hydrolyzes organophosphates, arylesters and lactones, whereas the lactones activity is assumed as the physio/pathological one. This study is aimed to predict the location of the PON1 active site within PON1 crystal structure, and the lactone structure suitability as PON1 ligand, by employing modeling techniques. Based on such calculations the ligands–PON1 interactions were characterized, and relating lactones rate of hydrolysis revealed an inverse correlation with the docking energy of the ligands–PON1 complex, and a direct correlation with the lactone side chain length. In conclusion, this study characterized the PON1 possible active site and proposes a tool which may make it possible to envisage the structure of potential endogenous and exogenous lactones such as the PON1 ligand.

© 2008 Elsevier Ltd. All rights reserved.

1. Introduction

Paraoxonase1 (PON1; EC 3.1.8.1), is a calcium dependent high-density lipoprotein (HDL) bound enzyme, synthesized in the liver and secreted into the blood stream. It has been demonstrated that many of the anti-atherogenic functions of HDL are attributed to its associated PON1.^{1–4} PON1 levels and activity have been shown to be regulated both genetically and by diet,^{5–7} and have decreased levels in hypercholesterolemic, diabetic, and cardio-vascular (CVD) patients.⁸ Despite the mass evidence for the anti-atherogenic roles of PON1, the precise biological activities that mediate these functions remain elusive, and the identity of its endogenous substrates is still unknown.

PON1 catalyzes the hydrolysis of multiple compounds such as organophosphates, arylesters, lactones, and hydroperoxides.^{9–12} It is speculated that the main PON1 substrates are lactones,^{13–15} including the reverse lactonization reaction,^{16,17} while the arylesterase and organophosphatase activities seem to be ancillary.¹⁸ Recently, the crystallographic structure of a PON1 variant was published.¹⁹ Based on the elucidation of the enzyme's crystallographic structure, the authors predicted the location of the PON1 active site within the enzyme three-dimensional structure. By using site directed mutagenesis, it was shown that the lactonase and arylesterase activities of PON1 are mediated by histidine (His) 115 and His134 dyad.²⁰

Modeling and docking techniques could be useful tools in structure-based drug design, in which the evaluated ligands are allowed to interact with the protein 3D structure, enabling the determination of the target and target–ligand complex nature.²¹ Similarly, docking calculations may predict the fitness of the evaluated ligand within the protein, where the shape is complementary of the binding site, considered to be rigid for the protein and flexible for the ligand.²²

The aims of this study were to predict the location of the PON1 active site within the complete PON1 variant crystal structure, to characterize its interactions with known ligands by employing modeling techniques, and to compare our findings with the enzyme's active site, as suggested by Harel et al.¹⁹ Furthermore, based on such modeling calculations and on data from the literature, that provides the rate of PON1 hydrolysis of various lactones; we aim to propose a tool, which may make it possible to predict the structure of potential endogenous/exogenous lactones such as the PON1 ligand. Such a tool may increase the likelihood of identifying the PON1 natural substrates and the PON1 biological function, under the assumption that indeed the natural substrates for PON1 are lactones.

2. Results and discussion

The mechanism of PON1's anti-atherogenic function and the identity of PON1's endogenous substrates still remain to be resolved. This study is aimed to contribute some additional information related to the possible enzyme active site and the

* Corresponding author. Tel.: +972 4695 3512; fax: +972 4694 4980.

E-mail address: vaya@migal.org.il (J. Vaya).

distinctiveness of the amino acids involved in it, as well as to propose tools that will predict the structure of lactones, the major type of compound under investigation as a PON1 substrate.

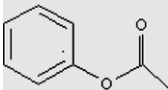
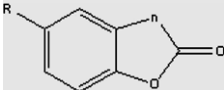
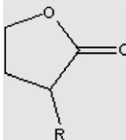
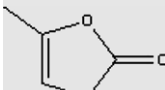
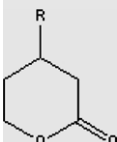
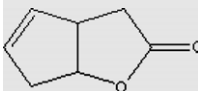
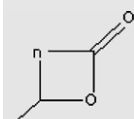
2.1. Prediction of the PON1 active site

PON1's crystal structure was adjusted and the substrates were constructed and docked on the enzyme crystallographic structure as described in Section 3. The ligands included in this study are presented in Table 1, which displays the calculated docked energy (DE) of the evaluated PON1 lactone complex, at its minimum level and the experimental rate of hydrolysis. It was observed that all of the lactones, which are known to be catalytically hydrolyzed by PON1, enter the same PON1 groove, and are, oriented very similarly one to the other, as shown in Figure 1A, and represented by dihydrocoumarin. The course of the carboxylate moiety of all these lactones within the enzyme's potential active site was in the same position, directed toward the inner part of the enzyme groove, forming a rigid conformation, while the residues attached to the lactone ring had more degrees of freedom facing the outer part of the edge of the enzyme groove.

2.2. Ligand–enzyme interactions

In a recent publication, Harel et al.,¹⁹ who predicted the PON1 active site based on the elucidation of the PON1 crystallographic structure, suggested the involvement of one calcium ion among the two atoms present (the catalytic Ca^{+2}) at the top of the central tunnel of the six bladed propeller shape of PON1. The second Ca^{+} (at the center of the tunnel) was predicted to have a structural function. It was suggested that the catalytic calcium ion interacts with asparagine (Asn)168, Asn270, Asn224, aspartic acid (Asp)269 and glutamic acid (Glu)53, while His115 and His134 are important for the hydrolysis mechanism.^{19,20} In this study, by performing docking analysis with the minimum DE of the complex PON1–ligand, we were able to allocate the possible PON1 active site and to compare the results with the above prediction. The summary of this analysis, which was carried out with ADT software—AutoDock, is shown in Figure 1B and demonstrates the various interactions between the ligand and its surrounding PON1 amino acids. Figure 1B shows that the Asn168 NH_2 residue and the His115 amine form hydrogen bonds with the ligand carbonyl oxygen, and the Asn224 NH_2 residue forms a hydrogen bond with the ligand carboxylate oxygen, thus facilitating the nucleophilic attack on the carbonyl carbon of

Table 1
The structure of lactones and phenyl acetate evaluated in this study for relating structure to activity

Structure	Name	Docking energy (DE)	Hydrolysis (μmol/min/mg)	
	Phenyl acetate	−6.7	112 ± 5	
	$n = 1, R = H$	−7.23	13.57 ± 1.03	
	$n = 2, R = H$	−7.83	12.99 ± 0.83	
	$n = 1, R = OH$	−6.83	32.95 ± 3.1	
	$R = H$	γ-Butyrolactone	−5.7	3.21 ± 0.27
	$R = CH_3$	γ-Valerolactone	−6.36	4.5 ± 0.37
	$R = CH_2CH_3$	γ-Hexalactone	−7.18	5.17 ± 0.42
	$R = CH_2CH_2CH_3$	γ-Heptalactone	−7.12	5.72 ± 0.23
	$R = (CH_3)CH_3$	γ-Octalactone	−6.99	6.92 ± 0.43
	$R = (CH_2)_4CH_3$	γ-Nonalactone	−7.87	14.47 ± 1.13
	$R = (CH_2)_5CH_3$	γ-Decanolactoe	−8.87	17.38 ± 1.47
	$R = (CH_2)_6CH_3$	γ-Undecanolactone	−9.22	12.76 ± 1.05
	α-Angelica lactone	−6.24	18.3 ± 1.6	
	$R = H$	δ-Valerolactotie	−6.17	67.1 ± 1.4
	$R = CH_3$	δ-Hexalactone	−6.97	7.2 ± 0.23
	$R = (CH_2)_3CH_3$	δ-Nonalactone	−7.28	15 ± 1.23
	$R = (CH_2)_4CH_3$	δ-Decanolactone	−8.94	25.1 ± 0.13
	$R = (CH_2)_5CH_3$	δ-Undecatiolactone	−9.6	28.70 ± 1.7
	$R = (CH_2)_6CH_3$	δ-Dodecanolactone	−8.23	9.65 ± 0.52
	(1S,5R)-Oxabicyclooctenone	−6.19	1.67 ± 0.11	
	(1R,5S)-Oxabicyclooctenone	−6.56	0.83 ± 0.05	
	$n = 1$	β-Hydroxybutyrolactone	−5.49	3.83 ± 0.05
	$n = 3$	ε-Caprolactone	−6.61	14.8 ± 0.48

In a separate column is shown the calculated docking energy using the AutoDock 3.0.5 Genetic-Algorithm (GA), and in the last column the experimental rate of hydrolysis of each lactone as published in the literature.^{9,13}

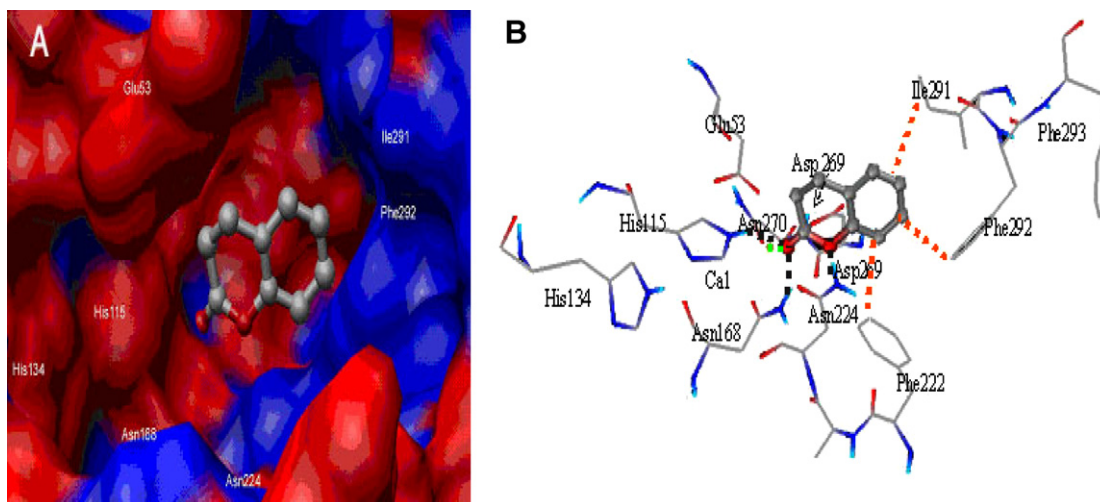


Figure 1. The orientation of dihydrocoumarin lactone within the PON1 potential binding site. (A) Molecular surface of PON1—hydrophilic (red) and hydrophobic (blue) zones docked with the dihydrocoumarin is shown. The groove, to which dihydrocoumarin is bound, is the predicted enzyme binding site. The carboxylate is directed toward the hydrophilic inner part of the enzyme groove, while the ligand's aromatic ring is facing the hydrophobic part of the groove (blue). (B) The dihydrocoumarin lactone with the lowest energy was docked into PON1. The negative, positive, and hydrophobic interactions of the ligand with the enzyme's amino acids are shown (red—oxygen, blue—nitrogen and gray—carbon). The carbonyl lactone oxygen forms hydrogen bonds with asparagine (Asn)168 and histidine (His)115, and the second lactone oxygen creates a hydrogen bond with Asn224, whereas the coumarin aromatic ring forms hydrophobic interactions with the phenylalanine (Phe)222 and 292 aromatic rings and with the isoleucine (Ile)291 side chain. Ligand–enzyme interactions are shown in dots (black—hydrogen bond, green—electrostatic, orange—hydrophobic).

the lactone ensuing with a ring opening and the formation of carboxylic acid. Therefore, the involvement of His115 in the mechanism of the catalysis may be mediated through its direct interaction with lactone substrates in the active site. The catalytic calcium of the enzyme is located at a distance of 1.93 Å from the lactone carbonyl oxygen, which allows for an electrostatic interaction between them, while the nitrogen atoms of Asn270 and Glu53 are both at a distance of over 4 Å from the lactone oxygen's (Table 2). As a result, they are not likely to create van der Waals forces or to be directly involved in the catalysis of the lactone hydrolysis. Together with Asp269, the two amino acids, Asn270 and Glu53, seem to contribute only to the active site structure. The distances of the ligand functional groups from the relevant amino acids surrounding them are presented in Table 2. It must be pointed out that the docking method has some limitation when it is applied to unbound structure, due to minor conformational changes that may occur in the protein upon its interaction with a substrate. Such possible changes were not taken into consideration in the above calculations.

Table 2

The amino acids within the PON1 potential active site and their interactions with the lactone (dihydrocoumarin) residues

Enzyme's amino acid	Moiety of the ligand	Distance (Å)	Type of interaction with the ligand
Ca ²⁺	O-Carbonyl	1.930	Electrostatic
Asn168	O-Carbonyl	1.885	Hydrogen bond
His115	O-Carbonyl	2.405	Hydrogen bond
Asn224	O-Ester	1.923	Hydrogen bond
Phe292	Aromatic ring (C6)	3.515	Hydrophobic
Ile291	Aromatic ring (C5)	3.427	Hydrophobic
Phe222	Aromatic ring (C7)	3.889	Hydrophobic
Glu53	O-Ester	4.490	None
Asn270	O-Carbonyl	4.143	None
Asn270	O-Ester	5.970	None

The types of the interactions were deduced from the distance between the elements forming the interaction by means of the AutoDock program.

2.3. Lactone rates of hydrolysis versus their calculated docking energy

The crystal structure of PON1 was enabled to combine with the PON1 substrates using the AutoDock Tools (ADT) program, as described in Section 3. Recent evidence implies that PON1's native activity is of a lactonase nature. PON1 has been shown to hydrolyze over 30 different lactones.^{9,13} The impairment of PON1 lactonase activity (by substituting His115 and His134 with glutamines) led to the demising of several of the enzyme's anti-atherogenic properties.⁸ For example, PON1 mediated the inhibition of low-density lipoprotein oxidation and the stimulation of macrophage cholesterol efflux. PON1 is believed to primarily act as a lactonase, based also on the evolutionary relationship among the close family members (PON1, PON2, and PON3). PON2 has a limited spectrum of substrates with a specificity only for lactones and is also the oldest member of this family.^{10,23} Several endogenous components (such as 6-phospho-D-gluconolactone, homogentisic acid lactone, 3',5'-cyclic GMP- [forming a lactone between a ribose and a phosphoric acid]) and drugs (such as statins, testolactone) have lactone structures. The catalytic hydrolysis of such lactone rings by PON1, if it occurs, can significantly modify the biological effects of these compounds. Relating the structure of these various possible substrates (phosphotriesters, esters, and lactones) to their rate of hydrolysis showed that lactone hydrolysis is not dependent on the pK_a of the departing group, and unlike all other substrates, lactones seem to differ in their K_m rather than their K_{cat} values.¹⁵ These findings, and the relatively high rates of hydrolysis measured with several lactones as substrates, imply that PON1 is in fact a lactonase.²⁰ Furthermore, the lactonase hypothesis of PON1 is also based on the ability of plasma purified PON1 and PON3, not only to hydrolyze lactones, but also to catalyze the reverse reaction and to lactonize a broad range of hydroxy acids, such as 5-hydroxy-6E,8Z,11Z,14Z-eicosatetraenoic acid (5-HETE) and 4-hydroxy-5E,7Z,10Z,13Z,19Z-docosahexaenoic acid (4-HdoHE).¹⁷ Thus, according to all the above supporting evidence, the main core of the PON1 active site is believed to be specific to lactones.¹³ In this study, 23 lactones and one aryylester (phenyl acetate) were selected. The lactones selected for these calculations are those known to be hydrolyzed

when incubated with PON1, and data related to their rate of hydrolysis are available.^{9,13} The structures of these lactones are presented in Table 1. They comprise different lactone ring sizes, for example, four (β), five (γ), six (δ) and seven (ϵ) member rings (such as β -hydroxy butyrolactone, γ -butyrolactone, δ -valerolactone, and ϵ -caprolactone, respectively). The lactone ring in these compounds is either fused to an aromatic ring (such as 2-coumaronone) or fused to an aliphatic five-membered ring (such as oxabicyclooctenone). They may be saturated (such as γ -valerolactone) or unsaturated (such as α -angelicolactone). The lactone ring can be non-substituted (such as δ -valerolactone) or substituted with aliphatic chains of various lengths, from one to seven carbons (such as δ -hexalactone or δ -dodecanolactone, respectively). Phenyl acetate, an ester with a non-lactone structure, was also included in this study, because it is one of the major substrates occasionally used to assay PON1 activity.

Harel et al.¹⁹ postulated that both poor and effective substrates bind to the active site with similar affinity and that the differences in the hydrolysis rate lay in the mode of binding (position relative to the catalytic Ca^{2+} and the catalytic base). Results in Figure 2 indicate an inverse correlation (Eq. 1) between the lactone rate of hydrolysis and the DE (lower DE represents stronger enzyme–substrate interactions) with $R^2 = 0.7008$ ($P < 0.0001$). They imply that different substrates have varying affinities for the enzyme, which directly correlate with the substrate rate of hydrolysis catalyzed by PON1, while their positions within the PON1 active site are very alike. Results presented in Figure 2 and summarized in Eq. 1 underline the utility of the docking technique as a tool for the first stage of screening of compounds from databases, to be tested as potential ligands.

$$y = -5.7x - 32.189 \quad (1)$$

It was demonstrated by Draganov et al. that six-membered ring lactones (δ -lactones) are more prone to hydrolysis than their five member (γ -lactone) counterparts.¹³ In this study, in agreement with the above findings, the DE calculation also revealed that δ -lactones had lower docking energies than the five-membered rings. For example, the experimental γ -decanolactone rate of hydrolysis is 17.38 ± 1.47 $\mu\text{mol}/\text{min}/\text{mg}$ protein and its calculated DE is -8.87 kcal/mol, whereas that of δ -undecanolactone is 28.7 ± 1.7 $\mu\text{mol}/\text{min}/\text{mg}$ protein and its DE is -9.6 kcal/mol. The experimental rate of hydrolysis of γ -lactones versus δ -lactone

was also compared with the calculated $\Delta\Delta H_f$ and with the activation energy (E_a). $\Delta\Delta H_f$ was calculated using semi-empirical calculation (MOPAC, PM3) by computation of the formation enthalpy (ΔH_f) of the carboxylic acid minus ΔH_f of the corresponding lactone, affording similar values for both types of lactones. For example, $\Delta\Delta H_{f(\delta\text{-hexalactone})} = -57.78$ kcal/mol versus $\Delta\Delta H_{f(\gamma\text{-valerolactone})} = -57.19$ kcal/mol. On the other hand, when the activation energy (E_a) of the transformation of the γ or δ -lactones to the corresponding carboxylic acid was calculated, using SADDLE technique (MOPAC, PM3) for locating transition state, different values were obtained for the two types of lactones, δ -lactones (δ -hexalactone) $E_a = 18.52$ kcal/mol versus $E_a = 22.43$ kcal/mol for γ -lactones (γ -valerolactone). Thus, it may be concluded that the higher rate of hydrolysis of the δ -lactones versus the γ -lactones is demonstrated from both, the lower DE of the δ -lactone–enzyme complex versus the γ -lactones, and from the lower activation energy needed to open δ -lactones ring versus the γ -lactones ring.

A comparison of unsaturation of the lactone ring (e.g., α -angelica lactone) versus the corresponding saturated compound revealed that despite the similarity in their calculated docking energies, the unsaturated lactone rate of hydrolysis is superior. These results could be explained in that, although the calculating DE of these two types of compounds is the same, the presence of a double bond in the lactone ring decreases ring chemical stability with a dissociation energy of -66.52 kcal/mol and E_a of 11.207 kcal/mol for angelica γ -lactone versus dissociation energy of -57.19 kcal/mol and E_a of 22.432 kcal/mol for its corresponding saturated compound (γ -valerolactone). Therefore, it may be understood that the higher rate of hydrolysis of the unsaturated lactone to its corresponding carboxylic acid is mainly due to its lower chemical stability and activation energy.

A correlation between the rate that PON1 catalyzes lactone hydrolysis relative to the length of the side chain residue on the lactone ring (the lipophilic side chain attached to the γ - or δ -carbon) revealed a strong inverse correlation, with a calculated DE (Eq. 2) and with an $R^2 = 0.8498$ ($P < 0.0001$) (Fig. 3), suggesting that the increased hydrophobicity of the side chain improves enzyme–lactone affinity, with the exception of δ -valerolactone. Thus, γ -undecanolactone has a calculated DE = -9.22 kcal/mol, whereas γ -decanolactone has a DE = -8.87 kcal/mol and γ -hexalactone heptalactone has a DE = -7.12 kcal/mol. These findings are in agreement with Draganov et al.'s findings¹³ that correlated the side chain carbon number with the rate of hydrolysis, showing the

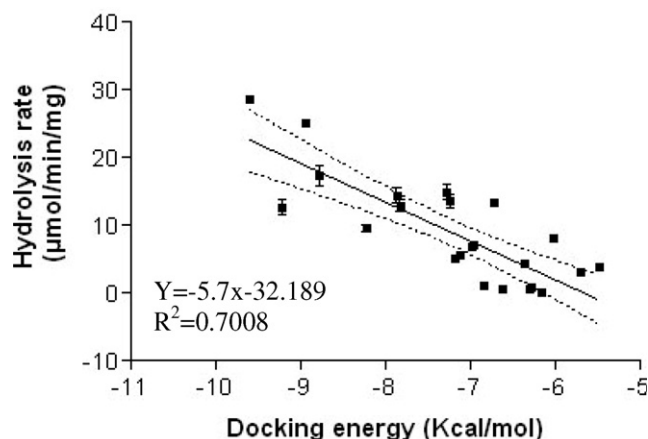


Figure 2. Calculated docking energies versus rate of PON1-catalyzed lactone hydrolysis. The PON1 crystallographic structure was acquired from the Protein Data Bank, and the calculated docking energies resulted from its interaction with different β -, γ -, δ -lactones and coumarins. By using AutoDock 3.0.5, the docking energies were plotted against the lactone rate of hydrolysis, as published in the literature.^{13,9} A line shows inverse correlation with $R^2 = 0.7008$ ($P < 0.0001$).

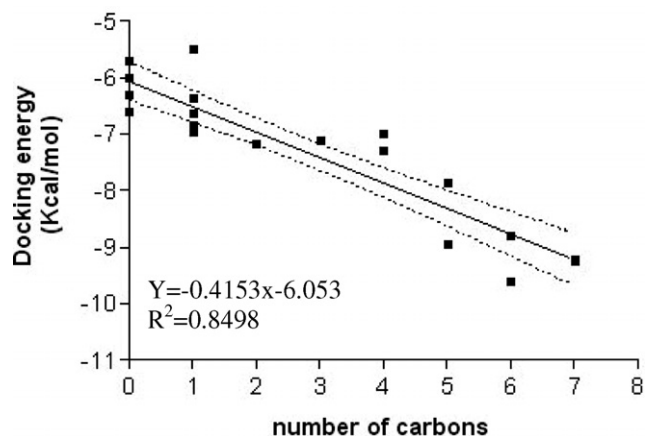


Figure 3. Calculated docking energies versus the number of carbons assembled on the lactone side chains. Ligands were first assigned their most stable configuration, using the Dundee PRODRG2 Server²¹, and then docked with the PON1 crystallographic structure, selecting the complex with the lowest energy level by means of the AutoDock 3.0.5. The line shows an inverse correlation between the calculated DE and the length of the aliphatic lactone side chains with $R^2 = 0.8498$ ($P < 0.0001$).

same, with the exception of δ -valerolactone. The calculated energy function in many circumstances correlates well with ligand size^{28,29} and in others with its bulkiness.²¹

$$y = -0.4513x - 6.053 \quad (2)$$

Our calculated docking energies of both γ -valerolactone and δ -valerolactone are close, -6.36 versus -6.17 kcal/mol, respectively, while their published rate of hydrolysis differs significantly (4.5 ± 0.37 vs 67.1 ± 1.4 μ mol/min/mg protein, respectively). Overlapping these two molecules in the PON1 active site revealed a minor distinction in their orientations, with only a 0.234 Å distance between the locations of their two-carboxylate oxygen's. It is not clear if such a distinction could explain the exceptionally high rate of hydrolysis of δ -valerolactone. In Figure 1, dihydrocoumarin is positioned in the enzyme active site exhibiting hydrophobic interactions (3.5 – 3.9 Å) of the lactone side chains, with mainly Phe222, Phe292 and Ile291 on the edge of the enzyme active site (Table 2). The aromatic ring moiety of the dihydrocoumarin is directed toward the phenylalanine aromatic ring and toward the 2-methyl butyl side chain of the isoleucine.

By using the same docking calculations technique, the interactions of lovastatin and spironolactone (both containing a lactone moiety) with the PON1 crystallographic structure were examined. It was observed that both cannot enter the enzyme predicted active site, but rather lovastatin was positioned on the enzyme's surface, forming non-specific interactions, whereas the spironolactone, as opposed to the other analyzed lactones, was positioned on the edge of the active site, with the lactone ring facing outside the groove far from the calcium ions (data not shown). These two drugs were initially thought to be hydrolyzed by PON1,⁹ but later it was found by Draganov et al.¹³ that the hydrolysis occurred as a result of the impurity, PON3, and not because of PON1. Interestingly, we have also analyzed how the docking of prulifloxacin, an active quinolone antibiotic with a carbonate ring, capable of being hydrolyzed by PON1,²⁴ would orient within the PON1 active site. Our results showed that this compound enters the same site as the hydrolyzable lactones, and the prulifloxacin carbonate moiety is positioned similarly to the lactone carboxylate moiety.

2.4. Rate of hydrolysis versus ligand dipole moment μ

Ligands were constructed and their configurations optimized to the minimum energy values by using a semi-empirical electronic structure calculation (MOPAC, PM3), as described in Section 3. The ligand total dipole moments were calculated, as well as the three components along the axis. Their values were correlated with the lactone rate of hydrolysis when catalyzed by PON1. It has been shown previously that the dipole moment of inhibitors within the tyrosinase active site correlates with the degree of the inhibition.²¹ In another investigation, the relative effectiveness of inhibitors and activators of the NAD-specific glutamate dehydrogenase was correlated with their dipole moment. It has been demonstrated that ligands with high dipole moment values were also good activators, while compounds with low dipole moments were inhibitors.²⁵ In this study, it was found that while no correlation was anticipated between the rate of hydrolysis and the total dipole moment, an inverse correlation (Eq. 3) between the published rates of hydrolysis of the lactones to their dipole moment on the Y-axis ($R^2 = 0.7064$) ($P < 0.0001$) was observed (Fig. 4). The dipole moment along the Y-axis seems to play an important role and to contribute to the partial charge of the lactone carbonyl carbon, and thus affects the rate of the nucleophilic attack on the carbonyl carbon. No such correlation was found between the lactone rate of hydrolysis and to the total μ or to the X- or Z-axis (data not shown).

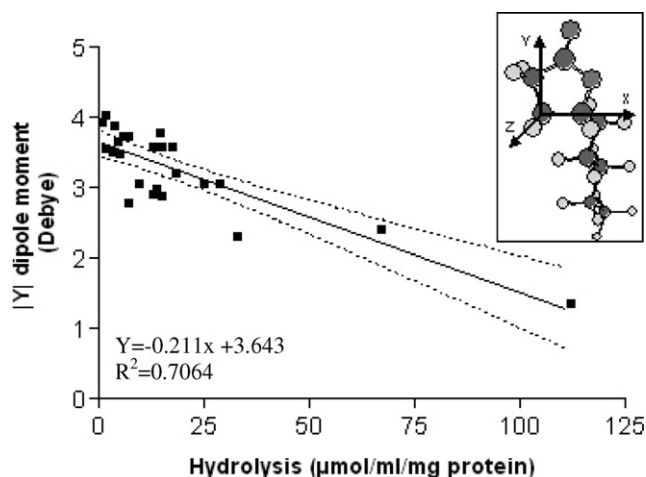


Figure 4. The rate at which PON1 catalyzes lactone hydrolysis versus the dipole moment on the Y-axis. Dipole moments on the Y-axis were calculated using the MOPAC program and the PM3 semi-empirical Hamiltonian. Values were plotted against lactone rates of hydrolysis by PON1, as published previously. Inverse correlation was anticipated with $R^2 = 0.7064$ ($P < 0.0001$). Inset: The X, Y and Z dipole moment axis of γ -nonalactone is oriented within the PON1 predicted active site, as attained upon MOPAC optimization. The other lactones form similar orientations. The Y-axis is directed toward the line connecting the lactone carbon 3 with the carbon 2, with a deviation from this line at an angle of 15.5° and a deviation of 11.27° from the lactone ring plan. The lactone side chain is basically directed toward the ($-Y$) axis. The molecule axis is calculated with internal coordinates, with carbon 3 at the origin (0,0,0).

$$y = -0.211x + 3.643 \quad (3)$$

We conclude that in this study, by using a modeling technique, a considerably different approach from the other two previous methodologies (crystallography and mutagenesis), the PON1 active site was also predicted, and the engagement of its amino acids in binding ligands, such as lactones, was depicted. Lactones of various structures were shown to fit such an active site, and by using docking calculations, their structure and experimental rate of hydrolysis were correlated with the DE of the complex PON1 ligand. Such a model may be useful as a tool, as an early filter, to better foresee a potential endogenous/exogenous PON1 ligand. Possibly, it could be utilized for screening databases of compounds, to predict the ability of specific lactones to be a PON1 substrate.

3. Experimental

3.1. Preparation of the protein

Crystal structure of the paraoxonase variant, prepared by directed evolution, was retrieved from the Protein Data Bank. The AutoDock Tools (ADT) program, an accessory program, that allows the user to interact with AutoDock^{26,27} from a graphical user interface, was used to manifest docking interaction between the proteins and its ligands. Water molecules were removed from the protein PDB file. Polar hydrogen atoms were added and Kollman united atomic charges assigned. The solvation parameters were included using the Addsol program (supplemented part of the ADT program). The 'C' letter of the calcium ions was changed to 'M', and the solvation parameters of the calcium ions were fixed.

3.2. Preparation of ligands

The ligands were constructed by 'CS ChemdrawPro' and 'CS ChemBats3DPro' and optimized to their minimum energy with the MOPAC program and the PM3 semi-empirical Hamiltonian.

The ADT program was assigned rotatable bonds and charges in the ligands. Alternatively, ligands were constructed using 'The Dundee PRODRG2 Server'.

3.3. Grid's parameters

The grid points were set to the catalytic site of the enzyme. The number of grid points in xyz was set to 60, 60, 60, the spacing value was equivalent to 0.375, and the grid center was set to 15.126, 21.269, 29.905. The calcium van der Waals parameters, which were obtained from the AutoDock program package, have an atom type M, equilibrium separation between the nucleus of the two calcium ions (distance between two calcium ions) $R_{ij} = 1.98 \text{ \AA}$, and pairwise potential energy (energy of interaction between two calcium ions) $\text{eps}_{ij} = 0.55 \text{ kJ/mol}$.

3.4. Docking

Ligand docking was carried out with the AutoDock 3.0.5 Genetic-Algorithm (GA). The approximate binding free energies calculated by this program are based on an empirical function derived by linear regression analysis of protein ligand complexes with known binding constants. This function includes terms for changes in energy due to van der Waals, hydrogen bonds, and electrostatic forces, as well as ligand torsion and desolvation. The docked energy also includes the ligand internal energy or the intra-molecular interaction energy of the ligand. All the parameters were assigned the default values, implemented by the program.

3.5. Analysis of results

All the docking results were visualized and analyzed with ADT and Chimera software. The lowest docked energy was taken as the best docked conformation of the compound for each macromolecule.

Acknowledgment

This study was supported by a grant from the Israel Science Foundation (ISF).

References and notes

1. Aviram, M.; Hardak, E.; Vaya, J.; Mahmood, S.; Milo, S.; Hoffman, A.; Billicke, S.; Draganov, D.; Rosenblat, M. *Circulation* **2000**, *101*, 2510.
2. Mackness, M. I.; Durrington, P. N.; Mackness, B. *Curr. Opin. Lipidol.* **2000**, *11*, 383.
3. Rozenberg, O.; Shih, D. M.; Aviram, M. *Arterioscler. Thromb. Vasc. Biol.* **2003**, *23*, 461.
4. Rosenblat, M.; Karry, R.; Aviram, M. *Atherosclerosis* **2006**, *187*, 74.
5. Aviram, M.; Kaplan, M.; Rosenblat, M.; Fuhrman, B. *Handb. Exp. Pharmacol.* **2005**, 263.
6. Costa, L. G.; Vitalone, A.; Cole, T. B.; Furlong, C. E. *Biochem. Pharmacol.* **2005**, *69*, 541.
7. Deakin, S. P.; James, R. W. *Clin. Sci. (Lond.)* **2004**, *107*, 435.
8. Rosenblat, M.; Gaidukov, L.; Khersonsky, O.; Vaya, J.; Oren, R.; Tawfik, D. S.; Aviram, M. *J. Biol. Chem.* **2006**, *281*, 7657.
9. Billecke, S.; Draganov, D.; Counsell, R.; Stetson, P.; Watson, C.; Hsu, C.; La Du, B. N. *Drug Metab. Dispos.* **2000**, *28*, 1335.
10. Draganov, D. I.; La Du, B. N. *Naunyn Schmiedeberg's Arch. Pharmacol.* **2004**, *369*, 78.
11. Jakubowski, H. J. *Biol. Chem.* **2000**, *275*, 3957.
12. La Du, B. N. In *international encyclopedia International Encyclopedia of pharmacology Pharmacology and therapeutics*; Kalow, W., Ed.; Pergamon: New York, 1992; p 51.
13. Draganov, D. I.; Teiber, J. F.; Speelman, A.; Osawa, Y.; Sunahara, R.; La Du, B. N. *J. Lipid Res.* **2005**, *46*, 1239.
14. Gaidukov, L.; Rosenblat, M.; Aviram, M.; Tawfik, D. S. *J. Lipid Res.* **2006**, *47*, 2492.
15. Khersonsky, O.; Tawfik, D. S. *Biochemistry* **2005**, *44*, 6371.
16. Santanam, N.; Parthasarathy, S. *Atherosclerosis* **2007**, *191*, 272.
17. Teiber, J. F.; Draganov, D. I.; La Du, B. N. *Biochem. Pharmacol.* **2003**, *66*, 887.
18. Ahmed, Z.; Ravandi, A.; Maguire, G. F.; Emili, A.; Draganov, D.; La Du, B. N.; Kuksis, A.; Connelly, P. W. *Biochem. Biophys. Res. Commun.* **2002**, *290*, 391.
19. Harel, M.; Aharoni, A.; Gaidukov, L.; Brumshtein, B.; Khersonsky, O.; Meged, R.; Dvir, H.; Ravelli, R. B.; McCarthy, A.; Tokar, L.; Silman, I.; Sussman, J. L.; Tawfik, D. S. *Nat. Struct. Mol. Biol.* **2004**, *11*, 412.
20. Khersonsky, O.; Tawfik, D. S. *J. Biol. Chem.* **2006**, *281*, 7649.
21. Khatib, S.; Nerya, O.; Musa, R.; Tamir, S.; Peter, T.; Vaya, J. *J. Med. Chem.* **2007**, *50*, 2676.
22. Goodsell, D. S.; Morris, G. M.; Olson, A. J. *J. Mol. Recognit.* **1996**, *9*, 1.
23. La Du, B. N.; Aviram, M.; Billecke, S.; Navab, M.; Primo-Parma, S.; Sorenson, R. C.; Standiford, T. J. *Chem. Biol. Interact.* **1999**, *119–120*, 379.
24. Tougou, K.; Nakamura, A.; Watanabe, S.; Okuyama, Y.; Morino, A. *Drug Metab. Dispos.* **1998**, *26*, 355.
25. Bonete, M. J.; Perez-Pomares, F.; Ferrer, J.; Camacho, M. L. *Biochim. Biophys. Acta* **1996**, *1289*, 14.
26. Goodsell, D. S.; Olson, A. J. *Proteins* **1990**, *8*, 195.
27. Morris, G. M.; Goodsell, D. S.; Huey, R.; Olson, A. J. *J. Comput. Aided Mol. Des.* **1996**, *10*, 293.
28. Ferrara, P.; Gohlke, H.; Price, D. J.; Klebe, G.; Brooks, C. L., 3rd. *J. Med. Chem.* **2004**, *47*, 3032.
29. Pan, Y.; Huang, N.; Cho, S.; MacKerell, A. D., Jr. *J. Chem. Inf. Comput. Sci.* **2003**, *43*, 267.